

# A New Austenitic FeMnAlCrC Alloy with High-Strength, High-Ductility, and Moderate Corrosion Resistance

GowDong Tsay\*<sup>1</sup>, ChihLung Lin\*<sup>1</sup>, ChuenGuang Chao and TzengFeng Liu\*<sup>2</sup>

Department of Materials Science and Engineering, National Chiao Tung University,  
1001 Ta Hsueh Road, Hsinchu 30049, Taiwan, R. O. China

In this study, a new austenitic Fe-28%Mn-9%Al-6%Cr-1.8%C (in mass%) alloy is developed. Because the alloy contains a high density of fine (Fe,Mn)<sub>3</sub>AlC carbides within the austenite matrix, the alloy in the as-quenched condition exhibits an excellent combination of strength and ductility comparable to that of the aged FeMnAlC alloys. In addition, owing to the formation of a layer of Cr and Al oxides in the passive film formed on the alloys, the corrosion potential  $E_{\text{corr}}$  (-538 mV) and the pitting potential  $E_{\text{pp}}$  (-25 mV) of the present alloy in 3.5% NaCl solution are considerably higher than the  $E_{\text{corr}}$  (-920~-789 mV) and  $E_{\text{pp}}$  (-500~-240 mV) values of the as-quenched and aged FeMnAlC alloys. Whereas the tensile strength of the present alloy is almost the same as that of conventional AISI 410 martensitic stainless steel, the present alloy possesses superior ductility than AISI 410 martensitic stainless steel. Furthermore, in 3.5% NaCl solution, the  $E_{\text{pp}}$  (-25 mV) of the present alloy is noticeably higher than that (-250~-100 mV) of the conventional AISI 410 martensitic stainless steel. These results indicate that the present alloy in the as-quenched condition can possess high-strength and high-ductility as well as moderate corrosion resistance.

[doi:10.2320/matertrans.M2010199]

(Received June 8, 2010; Accepted September 13, 2010; Published October 27, 2010)

**Keywords:** spinodal decomposition, carbides, mechanical properties, corrosion, iron manganese aluminum chromium carbon alloy

## 1. Introduction

Previous studies have shown that the as-quenched microstructure of the Fe-(28–34)%Mn-(7.8–10)%Al-(0–1.75)%M(M = Nb+V+Mo+W)-(0.85–1.3)%C alloys is single austenite ( $\gamma$ ) phase or  $\gamma$  phase with small amounts of (Nb,V)C carbides.<sup>1–10</sup> Depending on the chemical composition, the ultimate tensile strength (UTS), yield strength (YS), and elongation of the as-quenched alloys ranges from 840 to 950 MPa, 410 to 550 MPa and 70 to 57%, respectively.<sup>3–5</sup> Based on the results of the previous studies, it can be generally concluded that alloys having an optimal combination of strength and ductility can be obtained when the as-quenched alloys are aged at 550°C for about 16 h, this optimal combination is obtained because of the formation of fine (Fe,Mn)<sub>3</sub>AlC carbides ( $k'$  carbides) within the  $\gamma$  matrix and the absence of precipitates on the grain boundaries.<sup>5–8</sup> These alloys have an elongation better than about 30%, and UTS and YS values of 953~1259 MPa and 665~1094 MPa, respectively.<sup>5–9</sup> Although the austenitic FeMnAl(M)C alloys possess the remarkable combination of strength and ductility, the corrosion resistance of these alloys in aqueous environments is not adequate for use in industrial applications.<sup>1–15</sup> In order to improve the corrosion resistance, chromium has been added to the austenitic FeMnAlC alloys.<sup>14–17</sup> Consequently, it has been found that the corrosion resistance of the as-quenched Fe-(29.2–31.3)%Mn-(7.1–9.1)%Al-(2.8–6)%Cr-(0.88–1.07)%C alloys becomes considerably better than that of the as-quenched or aged FeMnAl(M)C alloys.<sup>14–17</sup> However, the as-quenched microstructure of these FeMnAlCrC alloys still remains to be single  $\gamma$  phase.<sup>14–17</sup> It is thus expected that the mechan-

ical strength of the as-quenched FeMnAlCrC alloys would be low similar to that of the as-quenched FeMnAl(M)C alloys. Furthermore, previous studies on the Fe-(28.3–30)%Mn-(8.7–9)%Al-(5–5.5)%Cr-(0.7–1)%C alloys aged at 550~600°C for a time period longer than 8 h have indicated that besides the formation of the fine  $k'$  carbides within the  $\gamma$  matrix, the coarse (Fe,Mn,Cr)<sub>7</sub>C<sub>3</sub> carbides might precipitate heterogeneously on the grain boundaries.<sup>18,19</sup> The precipitation of the coarse (Fe,Mn,Cr)<sub>7</sub>C<sub>3</sub> carbides on the grain boundaries results in the corrosion resistance being poor.<sup>16,17</sup> This implies that it is difficult for the austenitic FeMnAl(M)C and FeMnAlCrC alloys examined in the previous studies to possess both high-strength and high-ductility along with good corrosion resistance. Therefore, the main aim of this study is to develop new austenitic FeMnAlCrC alloys that possess high-strength and high-ductility as well as an appropriate corrosion resistance.

## 2. Experimental Procedure

In this study, the properties of five FeMnAlCrC alloys were investigated. Alloy A (0Cr) contained 28.1% Mn, 9.1% Al, 1.8% C, and balance Fe. Alloys B (3Cr), C (5Cr), D (6Cr), and E (8Cr) contained nearly the same amount of Mn, Al, and C, but contained different amounts Cr, i.e. 3.1, 5.0, 6.1 and 8.2%, respectively. The alloys were prepared in a vacuum induction furnace by using pure Fe, Mn, Al, Cr, and carbon powder. After being homogenized at 1250°C for 12 h under a protective argon atmosphere, the ingots were hot-rolled to a final thickness of 6 mm. The plates obtained after hot rolling were subsequently solution heat-treated at 1200°C for 2 h and then quenched rapidly into room-temperature water. The potentiodynamic polarization curves of the alloys were measured in 3.5% NaCl solution at 23°C by using an EG&G Princeton Applied Research Model 273 galvanostat/

\*1Graduate Student, National Chiao Tung University

\*2Corresponding author, E-mail: tfliu@cc.nctu.edu.tw; dir.mse93g@nctu.edu.tw

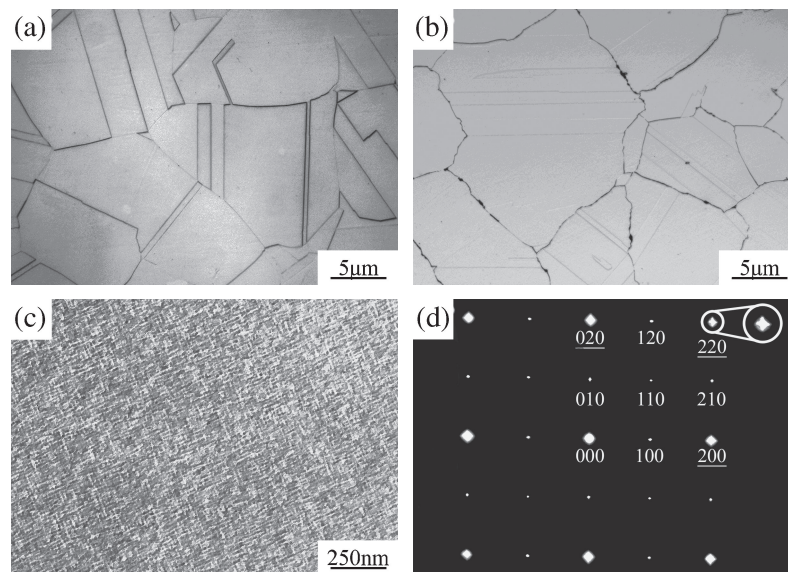


Fig. 1 Optical micrographs of present alloys: (a) alloy D (6Cr), and (b) alloy E (8Cr). Transmission electron micrographs of alloy D (6Cr): (c)  $(100)_{k'}$  DF, and (d) a selected area diffraction pattern taken from a mixed region covering the  $\gamma$  matrix and fine  $k'$  carbides. The zone axis is  $[001]$  ( $hkl$ :  $\gamma$  matrix;  $hkl$ :  $k'$  carbide).

potentiostat at a potential scan rate of  $5 \text{ mVs}^{-1}$ . The concentration of elements in the passive film formed on the surface of the alloys was examined by using a combined Auger electron spectroscopy (AES)/X-ray photoelectron spectroscopy (XPS)/secondary ion mass spectroscopy (SIMS) surface analysis system. The microstructures of the alloys were examined by optical microscopy and transmission electron microscopy (TEM). TEM specimens were prepared by using a double-jet electropolisher with an electrolyte containing 15% perchloric acid, 25% acetic acid, and 60% ethanol. Electron microscopy was carried out using JEOL-2100 transmission electron microscope operating at 200 kV. Tensile tests were performed at room temperature using an Instron tensile testing machine at a strain rate of  $5 \times 10^{-4} \text{ s}^{-1}$ . The specimens used for the tensile test were plates having a gauge length of 50 mm, width of 12 mm and thickness of 5 mm. The YS was measured at an offset strain of 0.2%, and the percent elongation was determined from the total elongation measured after fracture.

### 3. Results and Discussion

Optical micrography examinations indicated that the as-quenched microstructure of alloys A (0Cr) through D (6Cr) was essentially  $\gamma$  phase with annealing twins. A typical example is shown in Fig. 1(a). The micrograph indicates that Cr could be completely dissolved within the  $\gamma$  matrix at  $1200^\circ\text{C}$  for  $\text{Cr} \leq 6\%$ . However, when the Cr content was increased up to 8%, some precipitates were observed to be formed on the grain boundaries, as illustrated in Fig. 1(b). TEM examinations indicated that the precipitates on the grain boundaries were  $(\text{Fe,Mn,Cr})_7\text{C}_3$  carbides; these precipitates were similar to those observed by the present researchers in the as-quenched  $\text{Fe}-(29.2\text{--}30.2)\%\text{Mn}-(7.1\text{--}9.1)\%\text{Al}-(6.6\text{--}9.1)\%\text{Cr}-(0.94\text{--}1.07)\%\text{C}$  alloys.<sup>16,17</sup> TEM examinations also revealed that a high density of fine  $k'$  carbides was present within the  $\gamma$  matrix in all the alloys. The fine  $k'$  carbides

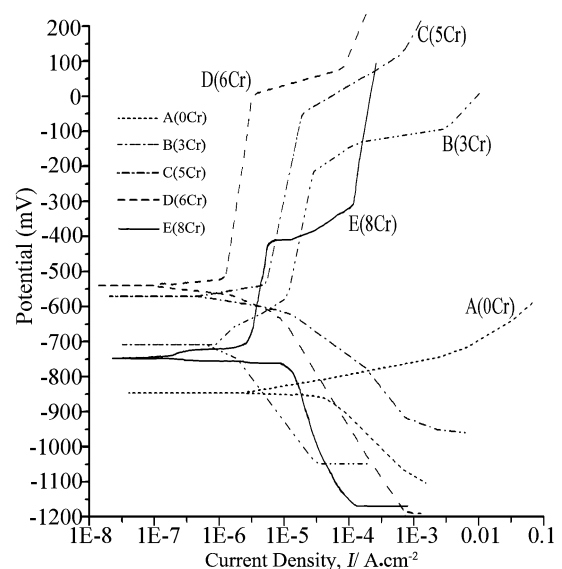


Fig. 2 Potentiodynamic polarization curves for present five alloys measured in 3.5% NaCl solution.

having an  $L'1_2$  (ordered f.c.c.) structure were formed by spinodal decomposition during quenching. An example is shown in Figs. 1(c) and 1(d). This result is similar to that obtained for the as-quenched  $\text{Fe}-(28\text{--}30)\%\text{Mn}-9\%\text{Al}-(1.8\text{--}2)\%\text{C}$  alloys.<sup>20,21</sup> Accordingly, besides the presence of the coarse  $(\text{Fe,Mn,Cr})_7\text{C}_3$  carbides on the grain boundaries in alloy E (8Cr), the as-quenched microstructure of alloys A (0Cr) through E (8Cr) was  $\gamma$  phase containing fine  $k'$  carbides.

Figure 2 shows the potentiodynamic polarization curves of the five alloys measured in 3.5% NaCl solution. A broad passive region can be clearly observed in the curves of all the alloys except in the curve of the alloy not containing Cr. In addition, the width of the passive region increased as the Cr content increased from 3 to 6%, and the width decreased

Table 1 Electrochemical parameters extracted from polarization curves and mechanical properties of present five alloys.

Alloy	Electrochemical parameters from polarization curves				Mechanical properties		
	$E_{\text{corr}}$ (mV)	$E_{\text{cr}}$ (mV)	$E_{\text{pp}}$ (mV)	$I_{\text{p}}$ ( $\text{A}\cdot\text{cm}^{-2}$ )	UTS (MPa)	YS (MPa)	El (%)
A (0Cr)	-846	—	—	—	1080	868	55.5
B (3Cr)	-710	-572	-223	1.5E-05	1092	876	47.2
C (5Cr)	-571	-524	-65	8.19E-06	1102	882	39.1
D (6Cr)	-538	-490	-25	9.12E-07	1122	902	36.5
E (8Cr)	-746	-652	-412	3.52E-06	984	835	22.6

$E_{\text{corr}}$ , corrosion potential;  $E_{\text{cr}}$ , critical potential for active-passive transition;  $E_{\text{pp}}$ , pitting potential;  $I_{\text{p}}$ , passive current density, minimum value.

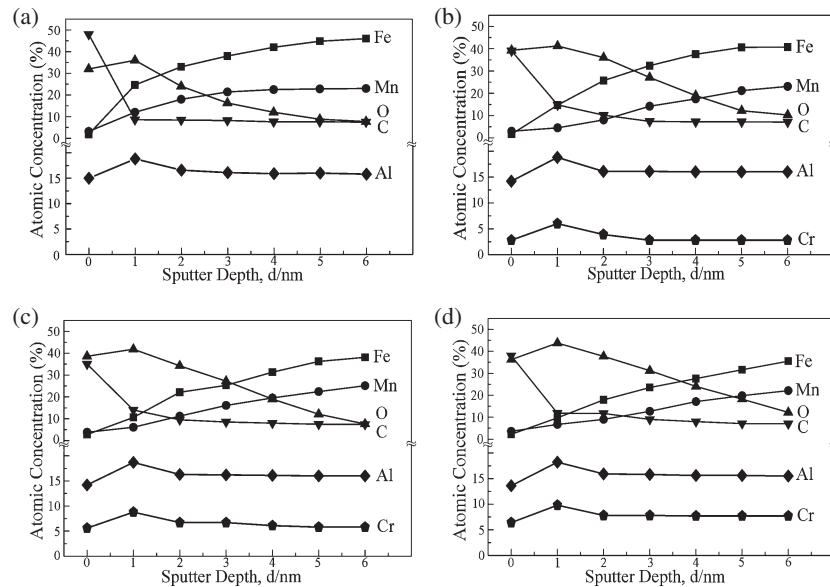


Fig. 3 AES depth profiles of passive film of present alloys: (a) A (0Cr), (b) B (3Cr), (c) D (6Cr), and (d) E (8Cr).

as the Cr content increased further up to 8%. The characteristic electrochemical parameters extracted from the polarization curves are listed in Table 1. As the Cr content changed, the corrosion potential ( $E_{\text{corr}}$ ) of the alloys varied from  $-846$  to  $-538$  mV. Alloy D (6Cr) exhibited the noblest  $E_{\text{corr}}$  ( $-538$  mV). Similarly, as the Cr content increased from 3 to 6%, the pitting potential ( $E_{\text{pp}}$ ) drastically increased from  $-223$  to  $-25$  mV. However, when the Cr content was increased further up to 8%,  $E_{\text{pp}}$  became more negative ( $-412$  mV). This indicated that alloy D (6Cr) had the highest resistivity to pitting damage. Figures 3(a)–(d) show the Auger depth profiles of the passive film formed on alloys A (0Cr), B (3Cr), D (6Cr), and E (8Cr), respectively. As can be clearly seen in these figures, broad peaks of Cr, Al, and O were observed at a depth of 0–2 nm in alloys B (3Cr), D (6Cr), and E (8Cr) alloys. The presence of a layer of Cr and Al oxides in the passive film may play an important role in improving the corrosion resistance characteristics of alloys B (3Cr) through D (6Cr). However, the formation of the coarse Cr-rich (Fe,Mn,Cr)<sub>7</sub>C<sub>3</sub> carbides resulted in a drastic decrease in the  $E_{\text{corr}}$  and  $E_{\text{pp}}$  values of alloy E (8Cr). As expected, the experimental results presented above were similar to those obtained for the as-quenched Fe-(29.2–30.2)%Mn-(7.1–9.1)%Al-(0–9.1)%Cr-(0.94–1.07)%C alloys.<sup>18,19)</sup>

The tensile properties of the five as-quenched alloys investigated in the present study are also listed in Table 1. It

can be clearly seen from the table that the UTS, YS, and elongation of alloy A (0Cr) were 1080 MPa, 868 MPa, and 55.5%, respectively. As the Cr content increased from 3 to 6%, the tensile strength slightly increased. Alloy D (6Cr) possessed the highest UTS (1122 MPa) and YS (902 MPa) with a good elongation of 36.5%. Owing to the high density of fine  $k'$  carbides within the  $\gamma$  matrix, alloys A (0Cr) through D (6Cr) in the as-quenched condition could possess a remarkable combination of strength and ductility. This result is similar to that reported for the Fe-28%Mn-9%Al-1.8%C alloy.<sup>21)</sup> However, when the Cr content was increased up to 8%, both the strength and elongation drastically reduced because of the formation of the coarse (Fe,Mn,Cr)<sub>7</sub>C<sub>3</sub> carbides on the grain boundaries.

On the basis of the above observations, three important experimental results are obtained as discussed below. (I) A comparison of the results of this study with those of previous studies, revealed that the yield strength of alloy D (6Cr) was not only superior to that (410–550 MPa) of the as-quenched Fe-(28–34)%Mn-(7.8–10)%Al-(0–2.8)%Cr-(0–1.75)%M(M = Nb+V+Mo+W)-(0.85–1.3)%C alloys but also comparable to that (665–1094 MPa) of the aged alloys.<sup>3–9,11–15)</sup> In addition, the  $E_{\text{corr}}$  and  $E_{\text{pp}}$  values of the alloys measured in 3.5% NaCl solution in previous studies were in the range of  $-920$  to  $-789$  mV and  $-500$  to  $-240$  mV, respectively.<sup>11–15)</sup> Owing to the presence of a layer of Al and Cr oxides in the passive

film, the  $E_{\text{corr}}$  and  $E_{\text{pp}}$  values of alloy D (6Cr) drastically increased to  $-538$  mV and  $-25$  mV, respectively. Therefore, it was concluded that the as-quenched alloy D (6Cr) possessed a better combination of high-strength, high-ductility, and moderate corrosion resistance. (II) The corrosion resistances of the present alloys in 3.5% NaCl solution were similar to those of the as-quenched Fe-(29.2–30.2)%Mn-(7.1–9.1)%Al-(3–9.1)%Cr-(0.94–1.07)%C alloys.<sup>16,17)</sup> This implied that the presence of the fine  $k'$  carbides within the  $\gamma$  matrix did not considerably affect the electrochemical behavior of the alloy in 3.5% NaCl solution. (III) The FeMnAlC alloy system was initially developed with the intention of replacing the conventional FeNiCr stainless steels because of its high strength, good toughness, low density, and low cost. However, previous studies revealed that the FeMnAlC alloys exhibited poor corrosion resistance in aqueous environments.<sup>11–15)</sup> It is interesting to note that the characteristics of alloy D (6Cr) are similar to those of the conventional martensitic stainless steels, conventional martensitic stainless steels are commonly used for manufacturing components that require a combination of high strength and moderate corrosion resistance.<sup>22)</sup> AISI 410 (12%Cr-0.10%C) is an example of martensitic stainless steels.<sup>22)</sup> Therefore, in the following description, we will compare the properties of AISI 410 and alloy D (6Cr). The high strength and moderate corrosion resistance of the AISI 410 can be achieved by carrying out heat treatment, including austenitizing, air-quenching and tempering treatments.<sup>22)</sup> After being tempered at a temperature between 250 and 593°C, the UTS, YS, and elongation were found to be 827~1337 MPa, 724~1089 MPa, and 20~17%, respectively.<sup>22)</sup> Additionally, the  $E_{\text{corr}}$  and  $E_{\text{pp}}$  values of AISI 410 measured in 3.5% NaCl solution ranged from  $-675$  to  $-312$  mV and  $-250$  to  $-100$  mV, respectively.<sup>23–25)</sup> The mechanical strength of alloy D (6Cr) was comparable to that of AISI 410, and alloy D exhibited better elongation than AISI 410. In addition, the  $E_{\text{pp}}$  value ( $-25$  mV) of alloy D (6Cr) was much higher than that ( $-250$ ~ $-100$  mV) of AISI 410. This might be attributed to the fact that although AISI 410 might have a Cr content of up to about 12%, a large amount of coarse Cr-rich (Fe,Cr)<sub>23</sub>C<sub>6</sub> carbides precipitate within its martensitic matrix during tempering. The precipitation causes the Cr concentration, which is dependent on the Cr-rich carbides, to reduce considerably, and hence, the boundaries between the carbides and the martensitic matrix act as locations for nucleation and as anodic positions for pitting corrosion.<sup>26,27)</sup> Therefore, the pitting potential of the tempered AISI 410 decreases considerably. In contrast to the tempered AISI 410, there was no evidence of the formation of chromium carbides in the as-quenched alloy D (6Cr). Furthermore, the average particle size of the fine  $k'$  carbides was only about 22 nm. In addition, the fine  $k'$  carbide had the same crystal structure and a similar lattice parameter as the  $\gamma$  matrix, therefore, the interface between the  $k'$  carbide and the  $\gamma$  matrix was completely coherent. Consequently, even at a considerably low Cr content, the pitting potential of alloy D (6Cr) was noticeably higher than that of the tempered AISI 410.

#### 4. Conclusions

In this study, a new austenitic Fe-28%Mn-9%Al-6%Cr-1.8%C alloy is developed. The as-quenched alloy possesses a remarkable combination of high-strength, high-ductility, and moderate corrosion resistance, which is attributed to the presence of fine  $k'$  carbides formed coherently within the  $\gamma$  matrix during quenching and to a layer of Cr and Al oxides in the passive film. The pitting potential  $E_{\text{pp}}$  ( $-25$  mV) of alloy D (6Cr) measured in 3.5% NaCl solution is noticeably higher than that of the aged FeMnAlC alloys ( $-500$ ~ $-240$  mV) and the tempered AISI 410 martensitic stainless steel ( $-250$ ~ $-100$  mV). In addition, the tensile strength of alloy D is comparable to that of the aged FeMnAlC alloys and AISI 410.

#### Acknowledgments

This work was supported by the National Science Council, Taiwan (NSC-97-2221-E-009-027-MY3).

#### REFERENCES

- 1) C. N. Hwang, C. Y. Chao and T. F. Liu: *Scr. Metall.* **28** (1993) 263–268.
- 2) C. N. Hwang and T. F. Liu: *Scr. Mater.* **36** (1997) 853–859.
- 3) S. C. Tjong and S. M. Zhu: *Mater. Trans.* **38** (1997) 112–118.
- 4) I. S. Kalashnikov, O. Akselrad and M. S. Khadyev: *Metal Sci. Heat Treat.* **48** (2006) 219–225.
- 5) W. K. Choo, J. H. Kim and J. C. Yoon: *Acta Mater.* **45** (1997) 4877–4885.
- 6) I. Kalashnikov, O. Acelrad, A. Shalkevich and L. C. Pereira: *J. Mater. Eng. Perform.* **9** (2000) 597–602.
- 7) G. S. Krivonogov, M. F. Alekseyenko and G. G. Solov'yeva: *Fiz. Metal. Metalloved.* **39** (1975) 775–781.
- 8) I. S. Kalashnikov, O. Acelrad, A. Shalkevich, L. D. Chumakova and L. C. Pereira: *J. Mater. Process Tech.* **136** (2003) 72–79.
- 9) I. S. Kalashnikov, B. S. Ermakov, O. Akselrad and L. K. Pereira: *Metal Sci. Heat Treat.* **43** (2001) 493–496.
- 10) K. H. Han: *Mater. Sci. Eng. A* **279** (2000) 1–9.
- 11) M. Ruscak and T. P. Perng: *Corrosion* **51** (1995) 738–743.
- 12) W. T. Tsai, J. B. Duh and J. T. Lee: *J. Mater. Sci.* **22** (1987) 3517–3521.
- 13) J. B. Duh, W. T. Tsai and J. T. Lee: *Corrosion* **44** (1988) 810–818.
- 14) S. C. Chang, J. Y. Liu and H. K. Juang: *Corrosion* **51** (1995) 399–406.
- 15) C. J. Wang and Y. C. Chang: *Mater. Chem. Phys.* **76** (2002) 151–161.
- 16) C. S. Wang, C. Y. Tsai, C. G. Chao and T. F. Liu: *Mater. Trans.* **48** (2007) 2973–2977.
- 17) Y. H. Tuan, C. S. Wang, C. Y. Tsai, C. G. Chao and T. F. Liu: *Mater. Chem. Phys.* **114** (2009) 595–598.
- 18) Y. H. Tuan, C. L. Lin, C. G. Chao and T. F. Liu: *Mater. Trans.* **49** (2008) 1589–1593.
- 19) C. F. Huang, K. L. Ou, C. S. Chen and C. H. Wang: *J. Alloy. Compd.* **488** (2009) 246–249.
- 20) C. S. Wang, C. N. Hwang, C. G. Chao and T. F. Liu: *Scr. Mater.* **57** (2007) 809–812.
- 21) K. M. Chang, C. G. Chao and T. F. Liu: *Scr. Mater.* **63** (2010) 162–165.
- 22) J. R. Davis: *Stainless Steels*, (ASM International, OH, 1994) pp. 3–18.
- 23) U. M. Dawoud, S. F. Vanweele and Z. S-Smialowska: *Corr. Sci.* **33** (1992) 295–306.
- 24) N. Azzzerri, F. Mancia and A. Tamba: *Corr. Sci.* **22** (1982) 675–687.
- 25) C. X. Li and T. Bell: *Corr. Sci.* **48** (2006) 2036–2049.
- 26) C. T. Kwok, H. C. Man and F. T. Cheng: *Surface Coat. Tech.* **126** (2000) 238–255.
- 27) C. T. Kwok, K. H. Lo, F. T. Cheng and H. C. Man: *Surface Coat. Tech.* **166** (2003) 221–230.